PNAS RESEARCH ARTICLE | NEUROSCIENCE
PSYCHOLOGICAL AND COGNITIVE SCIENCES

Hippocampal contributions to novel spatial learning are both age-related and age-invariant

Li Zheng[a,1], Zhiyao Gao[b], Stephanie Doner[a], Alexis Oyao[a], Martha Forloines[c], Matthew D. Grilli[a,d], Carol A. Barnes[a,d], and Arne D. Ekstrom[a,d]

Edited by James Knierim, Johns Hopkins University, Baltimore, MD; received May 10, 2023; accepted October 30, 2023 by Editorial Board Member Emery N. Brown

Older adults show declines in spatial memory, although the extent of these alterations is not uniform across the healthy older population. Here, we investigate the stability of neural representations for the same and different spatial environments in a sample of younger and older adults using high-resolution functional MRI of the medial temporal lobes. Older adults showed, on average, lower neural pattern similarity for retrieving the same environment and more variable neural patterns compared to young adults. We also found a positive association between spatial distance discrimination and the distinctiveness of neural patterns between environments. Our analyses suggested that one source for this association was the extent of informational connectivity to CA1 from other subfields, which was dependent on age, while another source was the fidelity of signals within CA1 itself, which was independent of age. Together, our findings suggest both age-dependent and independent neural contributions to spatial memory performance.

spatial memory | remapping | aging | hippocampus | fMRI

Significance

Spatial memory declines with age, although some older adults show little cognitive decline, even into their 80s. One important lead for age-related changes comes from electrophysiological studies of older rats, who have less stable neural representations for a spatial environment, termed "place cells." Using high-resolution fMRI (functional MRI) targeting the human hippocampus, we demonstrate that older adults also have less stable neural representations within the same environment. Our results reveal, however, that there are both age and performance dependent differences driving these effects. While older adults, on average, showed alterations in information flow within the hippocampal circuit, better performing individuals showed more differentiated neural representations regardless of age. Together, these findings provide insight into the impact of age on spatial memory.

Numerous studies in rodents, nonhuman primates, and humans suggest that advanced age results in reduced spatial navigation performance and spatial memory declines compared to younger adults (1–4). Yet determining why such complex spatial memory difficulties (4) arise for many adults with advanced age has remained elusive. Single neuron recordings from rodents provide a potential lead, suggesting that some of these alterations may derive from differences in neural representations for spatial locations. For example, place cells in the CA1 subfield of the hippocampus show a reduction in the consistency of receptive field firing for the same environment (5, 6). This phenomenon, termed "remapping," may relate to the known spatial memory difficulties of older rats and potentially humans, although this idea so far is untested in older adults. In the CA3 subfield of the rodent hippocampus, old rat hippocampal representations do not strongly distinguish between two different environments (i.e., dedifferentiation) (7), suggesting a possible alteration in a computational mechanism termed "pattern separation" (8–10). This difficulty differentiating separate environments may relate more broadly to age-related network dedifferentiation in human and nonhuman primate studies (11–15), although this, too, has not been studied across the lifespan.

Remembering different places involves formation of distinct neural representations for different environments and reinstatement of the same neural representation for the same environment. Therefore, if older adults show impaired spatial memory, one prediction is that reinstated activity patterns for the same environment might show lower fidelity between similar experiences than that of younger adults. On the other hand, the reinstated neural pattern for older adults in a different environment may be less differentiated compared to that of younger adults (Fig. 1*D*). Here, we used high-resolution functional MRI (fMRI) targeting the hippocampus and other temporal lobe structures and employed multivariate pattern similarity (MPS) analyses. These analyses involve correlating the pattern of reinstated voxel activity within and between retrieved spatial environments. The hypothesis that decreases in older adult's spatial memory might arise from alterations in both environment-specific codes and differentiation of neural signals between environments was therefore tested. Based on previous work (5–7), we focused on hippocampus subfields CA1, CA2, and CA3/dentate gyrus (CA2/3/DG) for these analyses; additionally, we tested parahippocampus cortex (PHC), entorhinal cortex (ERC), perirhinal cortex (PRC), and subiculum (SUB) as other critical medial temporal lobe subareas and inputs into CA2/3/DG and CA1.

In younger adults, more differentiated and specific neural patterns (as measured using MPS with high-resolution fMRI) correlate with more accurate retrieval of spatial distances within spatial environments (16, 17). The relationship between spatial memory performance

Preprint Servers: Preprint at bioRxiv, DOI: 10.1101/2023.06.28.546918.

The authors declare no competing interest.

This article is a PNAS Direct Submission. J.K. is a guest editor invited by the Editorial Board.

[1]To whom correspondence may be addressed. Email: lizheng@arizona.edu.

This article contains supporting information online at https://www.pnas.org/lookup/suppl/doi:10.1073/pnas.2307884120/-/DCSupplemental.

Published December 6, 2023.

and hippocampus subfield MPS, however, remains untested in older adults. Because older adults show individual differences in spatial memory with aging (18, 19), one possibility is that age-related differences in remapping may instead relate to poorer spatial memory, regardless of the age of the individual ("age-invariant"). For example, Schimanski et al. (2013) found that both older and younger rats with lower correlations in place cell representations in CA1 within the same environment also showed worse performance on the Morris watermaze (6). Alternatively, some age-related differences in remapping may also be "age-variant," such that even when more accurately retrieving spatial memories for an environment, older adults continue to show differences in neural patterns. We investigated the mechanistic basis for these predicted effects by testing how differences in the input to CA1 might differ with age. We also measured how the degree of signal differentiation was related to CA1 neural remapping. Together, these measures allow us to determine both how changes in the inputs to specific hippocampus subfields, and the fidelity of signals within a subfield, relate more broadly to remapping.

Results

Older Adults Show Lower and More Variable MPS when Retrieving the Same Environment Compared to Younger Adults. Younger and older adults learned two different spatial environments to criteria (*Methods*) and then retrieved the spatial distances of stores from these environments while undergoing high-resolution fMRI (Fig. 1). We performed MPS, which assays how similar the voxel patterns are between different conditions (in this case, environments), on correct trials to test our hypotheses (*Methods*). MPS was submitted to a linear mixed-effects model with condition (within-city/between-city), regions of interest (ROI, i.e., PHC, ERC, PRC, SUB, CA1, and CA2/3/DG), and group (old/young). The model showed a significant condition by ROI by group interaction [F (5, 974483) = 8.232, P < 0.001, *SI Appendix*, Table S1].

Consistent with our hypothesis, a simple main effects analysis revealed that within-city MPS was significantly greater than between-city MPS in CA1 for younger adults [F(1, 80.35) = 5.419, P = 0.022; Bayesian results: median = 0.0016, HDI (Highest Density Intervals) = (0.0008, 0.0025), pd (probability of direction) = 99.99%], but did not differ in older adults [F(1,130.93) = 0.447, P = 0.505; Bayesian results: median = –0.00003, HDI = (–0.0012, 0.0012), pd = 51.91%, Fig. 2*A*]. For younger adults, both within-city [t(41.6) = 4.587, P < 0.001; Bayesian results: median = 0.0045, HDI = (0.0029, 0.0061), pd = 100%] and between-city MPS [t(39.0) = 3.254, P = 0.002; Bayesian results: median = 0.0028, HDI = (0.0013, 0.0044), pd = 99.98%] were significantly higher than zero, whereas this was not observed among older adults [within-city MPS: t(52.5) = 0.720, P = 0.475; Bayesian results: median = 0.0004, HDI = (–0.0014, 0.0022), pd = 64.48%; between-city MPS: t(48.1) = 1.388, P = 0.171; Bayesian results: median = 0.0004, HDI = (–0.0014, 0.0022), pd = 66.40%]. Furthermore, within-city MPS was significantly lower in older adults than in younger adults [F(1,47.33) = 6.076, P = 0.017; Bayesian results: median = 0.0042, HDI = (0.0017, 0.0067), pd = 99.95%, Fig. 2*B*], while there were no significant differences between the two age groups for between-city MPS [F(1,43.77) = 1.205, P = 0.278; Bayesian results: median = 0.0025, HDI = (0.0001, 0.0048), pd = 97.86%, Fig. 2*C*]. We did not find this pattern in other hippocampus subfields or other medial temporal lobe (MTL) areas (i.e., younger > older MPS within but not between city; see *SI Appendix*, *Supplementary Note 2* and Fig. S1 for the results from other medial temporal lobe areas). Together, the findings for CA1 suggest reduced consistency for the same environment during retrieval in older adults, in line with past findings from rodent studies (5, 6).

Notably, spatial distance discrimination performance between older and younger adults differed, despite both groups beginning the experiment at criteria levels of spatial distance discrimination performance (*Methods*), with older adults performing, on average, worse than younger adults (*SI Appendix, Supplementary Note 1*).

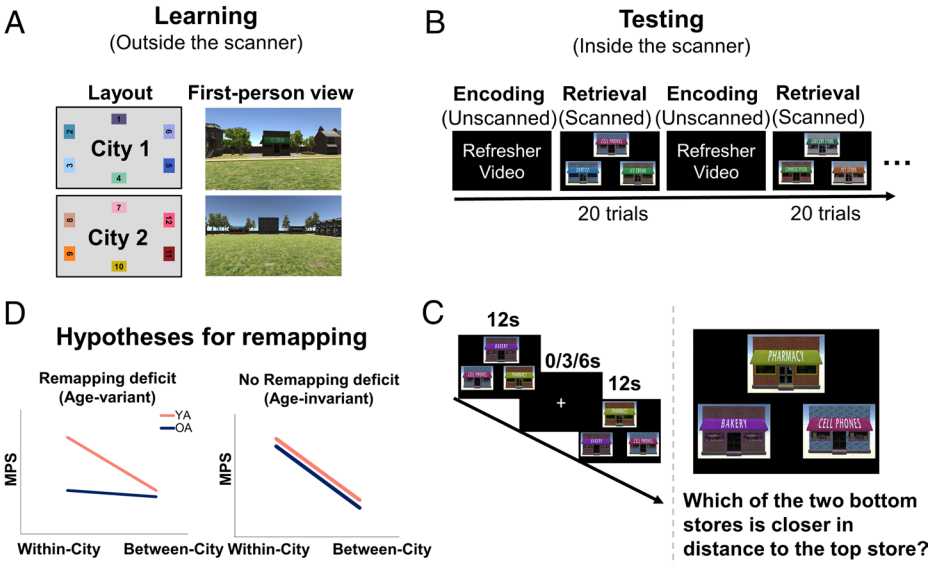

Fig 1. Schematic of the experimental design and hypotheses. (*A*) Layouts for each environment are depicted from an overhead view (*Left*) and first-person view (*Right*). Each colored box represents a target store. All participants experienced the environments through the first-person view. (*B*) Task structure in the MRI scanner. High-resolution fMRI scanning was only performed during retrieval and not encoding. The retrieval stage consisted of 6 runs of city-specific spatial distance discrimination, with three repeated runs per city. (*C*) Participants were asked to perform a space distance discrimination task during the retrieval stage. (*D*) Hypotheses, as laid out in the introduction: If older adults show impaired spatial memory, we should see alterations in the neural patterns for the same vs. a different environment (i.e., dedifferentiation: Within-city MPS is comparable with between-city MPS in older adults) as well as less specific reactivation of the same environment (i.e., reduced within-city MPS compared to younger adults). YA: younger adults, OA: older adults.

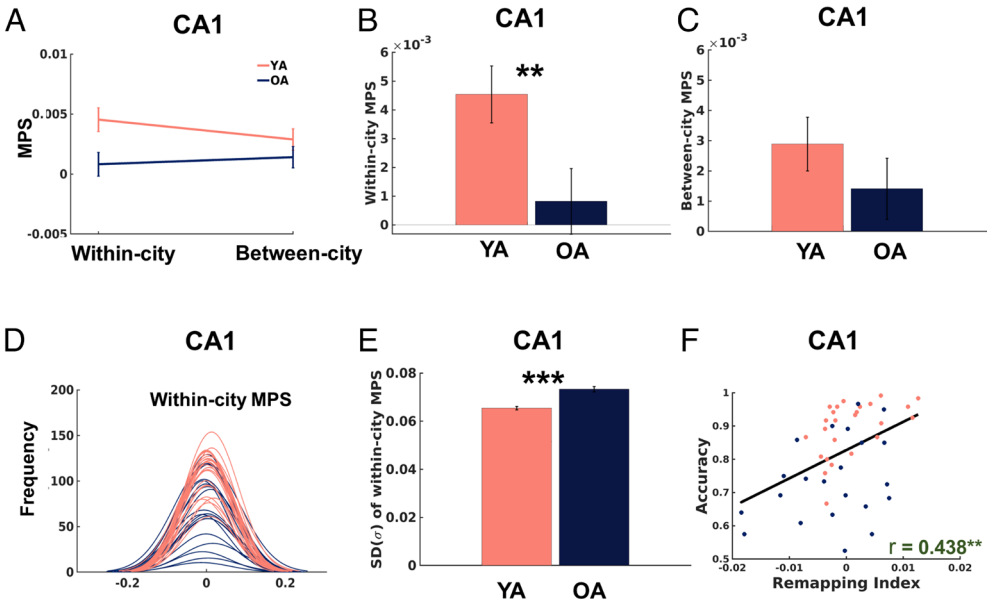

Fig 2. Differences in within- and between-city MPS. (*A*) Within-city MPS was significantly greater than between-city MPS in CA1 for younger adults but did not differ in the older adults. (*B*) The within-city MPS in CA1 was significantly lower in older adults than in younger adults. (*C*) The between-city MPS in CA1 was not significantly different in older and younger adults. (*D*) The distribution of within-city MPS in the CA1 of older adults (dark blue) was wider than younger adults (red). (*E*) Higher SD of within-city MPS in CA1 for older compared to younger adults. (*F*) The neural remapping index (within-city MPS minus between-city MPS) in CA1 was positively correlated with spatial distance discrimination performance ("accuracy"). Each individual dot represents data from an individual participant, with red dots representing younger adults, while dark blue dots represent older adults. Error bars represent the standardized errors of the means. All data reflect n = 25 for YA and n = 22 for OA independent participants. YA: younger adults, OA: older adults. $^{**}P < 0.01$ and $^{***}P < 0.001$.

Therefore, we used spatial distance discrimination performance and reaction time as covariates of no interest. Importantly, we found that the within > between MPS interaction effect survived controlling for spatial distance discrimination performance and reaction time. In addition, we found that the age differences in MPS for within > between city could not be accounted by differences in univariate activation levels, activation variance, gender, ROI volume, or greater shared perceptual similarity for within-city pairs (*SI Appendix*, Table S2 and *Supplementary Note 2*). In a control analysis, we reexamined all the aforementioned findings by including both correct and incorrect trials, which largely mirrored our findings with correct trials only (*SI Appendix, Supplementary Note 2*).

Why should older adults, on average, show a lower correlation in voxel patterns for the same environment, even on correct trials (the focus of our analyses)? One possibility is that the neural representations are less stable for the same environment, as suggested in past studies in rodents (5, 6). To address this issue, we first examined the stability of neural representations by visualizing the distribution of within-city MPS on correct trials. The MPS of older adults showed a wider distribution of values than younger adults, indicating a broader spread of activation patterns within a city (Fig. 2*D*). Direct comparison of younger vs. older adult within-city MPS revealed a larger SD for within-city MPS in CA1 of older individuals [$t(45) = 6.188$, $P < 0.001$, Cohen's D = 1.809; Fig. 2*E*]. The Bayes factor calculated for the SD for within-city MPS indicated extremely strong evidence against the null hypothesis ($BF_{10} = 66530.829$). This effect could not be accounted for by differences in performance when using spatial distance discrimination performance as a covariate in a linear regression model [$R^2_{adjusted} = 0.435$, $F(2, 44) = 18.734$, $P < 0.001$]. In control analyses, we reexamined the age differences in the SD of MPS when the number of trials was matched across the whole group and obtained similar results (*SI Appendix, Supplementary Note 2*). Together, the findings above suggested that older adults showed a lower mean within-city MPS and higher within-city MPS variance, regardless of performance.

Neural Remapping and Spatial Distance Discrimination Are Age-Invariant. Next, we asked how age and performance related to the mean differences in correlations within and between cities, which can be quantified using the "neural remapping index." A previous study from Kyle et al. (17) showed that better performing younger adults showed a greater difference for within- vs. between-city MPS (the neural remapping index). A higher score on this index indicated more differentiated environmental-specific neural representations (remapping) and a lower score indicated dedifferentiation or less distinct network patterns. Previous work has suggested that older adults and nonhuman primates show greater dedifferentiation for overlapping stimuli than do younger adults (11–15, 20). This may be particularly true for scenes, suggesting a parallel with navigation, although some studies have also supported the idea that these findings are age-invariant (21–23). In other words, better performing older adults could show comparable differentiation to younger adults, if the neural signals for the different environments are sufficiently differentiated.

Consistent with an age-invariant relationship between the neural remapping index and spatial distance discrimination, we found that the neural remapping index in CA1 was positively correlated with participant distance discrimination performance as measured by the percent of successfully retrieved distances of stores [$r(45) = 0.437$, $P = 0.002$, $BF_{10} = 17.830$, with strong evidence, Fig. 2*F*]. This correlation was age-invariant [after controlling for age, gender, and CA1 volume, the correlation persisted, i.e., $r_{partial}(45) = 0.405$, $P = 0.006$]. We did not find any correlation between the neural remapping index in other MTL subregions (Ps > 0.291, *SI Appendix*, Fig. S5*A* and *Supplementary Note 3*). Together, these findings suggest that better performing participants—regardless of age—showed greater differences in the CA1 remapping index.

Differences in the Neural Remapping Index Related to Spatial Distance Discrimination Are Mediated By Alterations in Input to CA1. We then investigated potential mechanisms for the age-invariant correlations between the neural remapping index and

spatial distance discrimination by considering how the neural signals in other MTL subregions might be contributing to this effect. Changes in connectivity are thought to underlie at least some age-related changes in hippocampus-mediated function (24). Reductions in the quality of input to CA1, for example, could result in less information available for local computations related to environment-specific codes. We quantified interregional informational connectivity using the values of the correlations of MPS between one subfield and another. Either higher or lower interregional connectivity was hypothesized as a plausible mechanism for reductions in input quality to CA1 (*Methods* and Fig. 3 *A* and *B*). We found that older adults showed increased interregional informational connectivity between PHC-ERC [t(45) = 2.467, Cohen's D = 0.721, $p_{corrected}$ = 0.03; BF_{10} = 3.172, with moderate evidence], PHC-CA1 [t(45) = 2.201, Cohen's D = 0.645, $p_{corrected}$ = 0.044; BF_{10} = 1.990, with anecdotal evidence], ERC-CA1 [t(45) = 4.249, Cohen's D = 1.242, $p_{corrected}$ = 0.001; BF_{10} = 207.124, with extremely strong evidence], ERC-CA2/3/DG [t(45) = 2.901, Cohen's D = 0.848, $p_{corrected}$ = 0.012; BF_{10} = 7.537, with moderate evidence], PRC-ERC [t(45) = 3.638, Cohen's d = 1.063, $p_{corrected}$ = 0.004; BF_{10} = 41.664, with very strong evidence], PRC-SUB [t(45) = 3.069, Cohen's D = 0.897, $p_{corrected}$ = 0.012; BF_{10} = 10.859, with strong evidence], PRC-CA1 [t(45) = 2.892, Cohen's D = 0.845, $p_{corrected}$ = 0.012; BF_{10} = 7.400, with moderate evidence], SUB-CA1 [t(45) = 3.018, Cohen's D = 0.882, $p_{corrected}$ = 0.012; BF_{10} = 9.716, with moderate evidence], and CA2/3/DG-CA1 [t(45) = 2.252, Cohen's D = 0.658, $p_{corrected}$ = 0.044; BF_{10} = 2.156, with anecdotal evidence, Fig. 3*D*]. Here, we specifically focused on the connections between input areas (i.e., PHC, ERC, PRC, SUB, and CA2/3/DG) to CA1 (Fig. 3*C*). We calculated the interregional informational connectivity by averaging across five selected connections: PHC-CA1, ERC-CA1, PRC-CA1, SUB-CA1, and CA2/3/DG-CA1 (*Methods* and Fig. 3*D*). We found a negative correlation between the interregional informational connectivity and spatial distance discrimination [r(45) = −0.500, P < 0.001; BF_{10} = 90.288, with very strong evidence, Fig. 3*E*] as well as interregional informational connectivity and the neural remapping index [r(45) = −0.407, P = 0.005; BF_{10} = 9.092, with moderate evidence, *SI Appendix*, Fig. S6*E*]. This suggests that a higher correlation between patterns in different subfields related to worse spatial distance discrimination and a lower neural remapping index.

To attempt to better understand the relationship between interregional informational connectivity, the neural remapping index, and spatial distance discrimination, we performed a mediation analysis. The model indicated that interregional informational connectivity (*SI Appendix*, Table S5) mediated the relationship between the neural remapping index in CA1 and spatial distance discrimination performance after controlling for CA1 volume and gender (Fig. 3*F*). Notably, when we entered age as a covariate, however, the mediation effect was no longer significant, suggesting that the interregional informational connectivity mediation effect was age-variant (*SI Appendix*, Table S5). Similar results were found when using other connectivity patterns to CA1 (ERC-CA1, PRC-CA1, SUB-CA1, and CA2/3/DG-CA1); see *SI Appendix*, Table S7 and *Supplementary Note 4* and *Methods*. We also examined the interregional informational connectivity between PRC-ERC, which has indirect connections with the CA1. The results suggest that PRC-ERC informational connectivity mediated the relationship between the neural remapping index in CA1 and spatial distance discrimination performance after controlling for CA1 volume and gender. This effect again did not survive after adding age as a covariate (*SI Appendix*, Table S9), indicating that the interregional informational connectivity mediation effect was age-variant. We found similar results when considering the correlation only for the same environment, suggesting that this effect may have been driven by the stability of patterns for the same environment (*SI Appendix, Supplementary Note 4*). Together, these

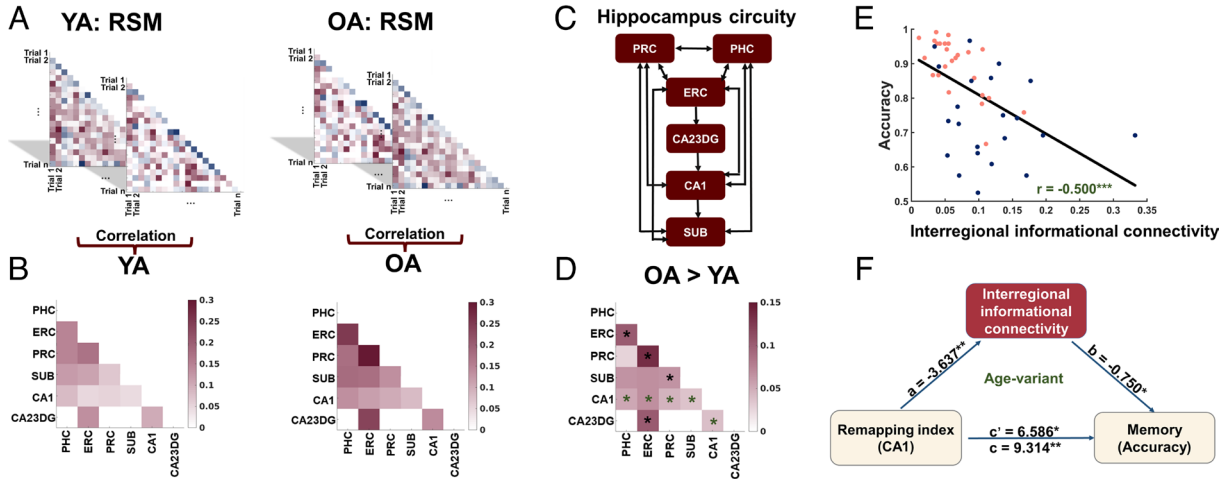

Fig 3. Differences in the neural remapping index related to spatial distance discrimination are mediated by alterations in input to CA1. (*A*) Schematic of interregional informational connectivity analysis. For each ROI, we calculated the pairwise Pearson correlation among the activation patterns of trials to obtain a T-trial by T-trial representational similarity matrix (RSM) for each group (*Left*: younger adults; *Right*: older adults). (*B*) A second-order representational similarity analysis was performed among the resulting RSMs for the 6 ROIs to obtain the informational connectivity matrix for each group (*Left*: younger adults; *Right*: older adults). (*C*) Hippocampus circuitry (adapted from "Differential connectivity of perirhinal and parahippocampal cortices within human hippocampal subregions revealed by high-resolution functional imaging" by Laura A. Libby, 2012). (*D*) Increased interregional informational connectivity in older adults from subfields with direct input to CA1 [the presence of asterisks (*) denotes statistical significance (P < 0.05, FDR corrected)] for interregional informational connectivity in older adults compared to younger adults. Specifically, green asterisks highlight direct connections to CA1, while black asterisks indicate indirect connections with CA1. (*E*) The interregional informational connectivity was negatively associated with spatial distance discrimination performance (accuracy). Each individual dot represents data from an individual participant, with red dots representing younger adults, while dark blue dots represent older adults. (*F*) Interregional informational connectivity mediated the relationship between the neural remapping index (i.e., within-city minus between-city MPS) in CA1 and spatial distance discrimination performance ("memory accuracy") after controlling for CA1 volume and gender, but this mediation effect was no longer significant after adding age as a covariate (i.e., age-variant). All data reflect n = 25 for YA and n = 22 for OA independent participants. YA: younger adults (red), OA: older adults (dark blue). *P < 0.05, **P < 0.01, and ***P < 0.001.

findings suggest that differences in the input to CA1 contribute to age-variant differences in the neural remapping index.

Correlations between the Neural Remapping Index and Spatial Distance Discrimination Are Mediated by Reduced CA1 Neural Consistency. We estimated the dimensionality of neural signals by performing principal component analysis (PCA) to determine whether the fidelity of signals within hippocampus subfields also contributed to variance in spatial distance discrimination performance. We measured the dimensionality using the number of PCs needed to explain 90% of the variance in voxel time course correlation patterns (Fig. 4*A* and *Methods*). The results showed that the dimensionality of CA1 was significantly lower in older adults compared to younger adults [t(45) = 4.327, Cohen's D = 1.265, P < 0.001; BF_{10} = 257.266, with extremely strong evidence, Fig. 4*B*]. To ensure the robustness of this effect, we performed several control analyses. We selected the top 50 voxels based on each participant's tSNR levels from CA1 (*Methods*) to confirm that the age differences we found were not influenced by differing numbers of voxels between individuals (*SI Appendix, Supplementary Note 5*). We also performed the PCA analysis using all voxels within individual participant's CA1 and matching the number of trials (*SI Appendix, Supplementary Note 5*). These analyses again revealed lower dimensionality in older adults than in younger adults in hippocampus subfield CA1 (*SI Appendix, Supplementary Note 5*).

We found that CA1 dimensionality was positively associated with spatial distance discrimination [r(45) = 0.803, P < 0.001; BF_{10} = 911,300,000, with extremely strong evidence, Fig. 4*C*]. Additionally, CA1 dimensionality was also positively correlated with the neural remapping index [r(45) = 0.538, P < 0.001; BF_{10} = 291.942, with extremely strong evidence, *SI Appendix*, Fig. S7*A*]. These effects were significant even after controlling for age, gender, and CA1 volume [spatial distance discrimination: rpartial(45) = 0.722, P < 0.001; neural remapping index: rpartial(45) = 0.495, P < 0.001], suggesting age-invariant effects. As discussed earlier, we also found a correlation between spatial distance discrimination and the neural remapping index in CA1 (Fig. 2*F*). Thus, we then ran an analysis to determine whether the number of extracted PCs in CA1 mediates this effect. This analysis indicated that the dimensionality of CA1 mediated the correlation between the neural remapping index and spatial distance discrimination, even after controlling for CA1 volume and gender (*SI Appendix*, Table S15).

The mediation effect remained significant when age was included as a covariate, suggesting that these effects were age-invariant (Fig. 4*D* and *SI Appendix*, Table S15 and *Supplementary Note 5*). These findings suggest that reduced fidelity of signals within CA1 mediated the relationship between the neural remapping index and participants' memories for the distances of landmarks to each other in each city. While we did identify positive correlations between spatial distance discrimination and dimensionality in other MTL subregions [rs > 0.798, ps < 0.001, FDR (false discovery rate) corrected], we did not observe any significant correlations between the neural remapping index in other MTL subregions and dimensionality (ps > 0.08, FDR corrected), nor did we find any evidence of mediation effects in other MTL subregions (*SI Appendix, Supplementary Note 5*). Therefore, increased neural differentiation between different cities was related to better spatial distance discrimination performance, based on the fidelity of signals within CA1—regardless of age.

Discussion

Our study focused on exploring the neural mechanisms underlying spatial memory decline in normative aging and how it might relate to well-documented changes in age-related hippocampus remapping in rodents. Because the neural representations within an environment should be more similar than those between environments, we subtracted the between-city pattern similarities from the within-city pattern similarities (generating the neural remapping index). We found that this index and spatial distance discrimination were positively correlated (Fig. 2*F*), reminiscent

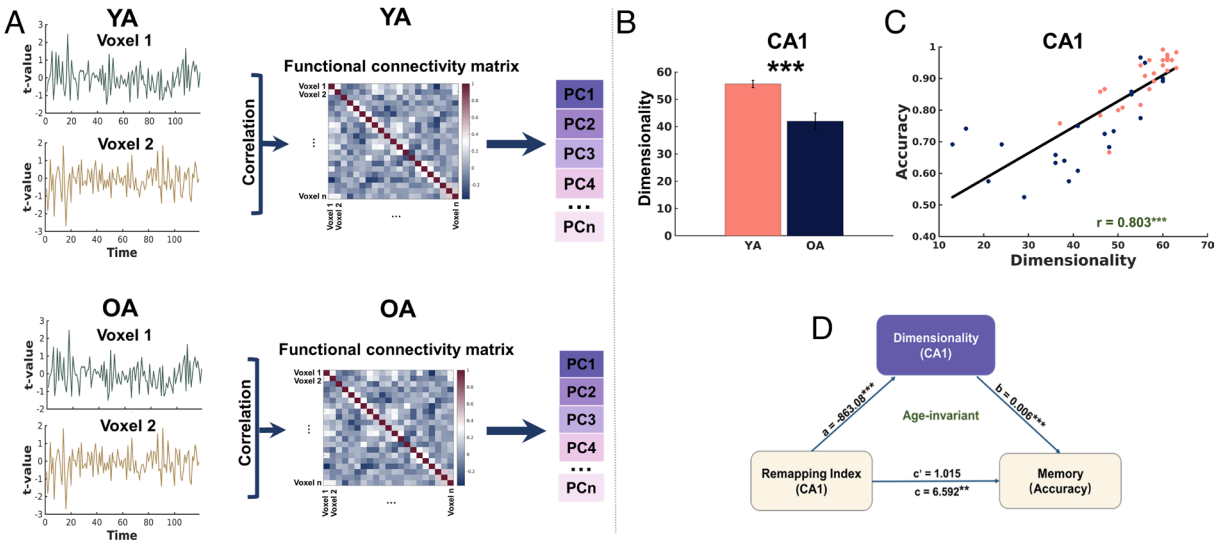

Fig 4. Correlations between the neural remapping index and spatial distance discrimination performance are mediated by reduced CA1 neural consistency. (*A*) Schematic of PCA: For each ROI, a series of *t*-statistics for each voxel of all correctly retrieved trials were extracted, and then used to calculate pairwise Pearson correlations, resulting in a functional connectivity matrix of N-voxel by N-voxel for each group (*Top*: younger adults; *Bottom*: older adults). PCA was then applied to the resulting N by N functional connectivity matrix to obtain PCs. (*B*) Reduced CA1 neural consistency in older adults. (*C*) The dimensionality of CA1 was positively associated with spatial distance discrimination performance (accuracy), even after controlling for age, gender, and CA1 volume. Each individual dot represents data from an individual participant, with red dots representing younger adults, while dark blue dots represent older adults. (*D*) The dimensionality of CA1 based on the PCA analysis fully mediated the effect of the neural remapping index (i.e., within minus between MPS) on spatial distance discrimination performance (memory accuracy), even after controlling for age, gender, and CA1 volume. Error bars represent the standardized errors of the means. All data reflect n = 25 for YA and n = 22 for OA independent participants. YA: younger adults, OA: older adults. PCs: principal components. **P < 0.01 and ***P < 0.001.

of the correlations found between CA1 remapping and spatial memory performance in rodents (5, 6). We found that one source of explained variance for this association was the extent of informational connectivity to CA1 from other subfields, which mediated the relationship of spatial distance discrimination performance and the neural remapping index yet was not present when controlling for age (Fig. 3*F*). A second source of variance in spatial distance discrimination performance was the fidelity of signals within CA1 itself, as measured by a PCA, which partially accounted for worse performance and lower neural remapping index values (Fig. 4*D*). A mediation analysis that persisted even after controlling for age suggested this effect was age-invariant. Thus, spatial memory changes in older adults appear to occur for at least two reasons. Among these are changes in the quality of input to CA1, which differs based on age, and the other is related to the fidelity of signals within hippocampus CA1, which is independent of age.

Previous research using high-resolution resting-state fMRI has found that there are no significant differences in patterns of functional connectivity between younger and older adults within the hippocampus subfields (25). Our task-based functional connectivity analysis using the *t*-statistic time series method (*SI Appendix, Supplementary Note 6*) also found no differences in connectivity patterns between the age groups. However, the interregional informational connectivity approach employed here (*Methods*) allowed us to assess the extent to which two brain regions communicate similar or different information based on the similarity of voxel patterns between subfields (26). More similar voxel patterns between subfields that provide input to CA1 in older adults would result in reduced informational transfer to this subfield. This, in turn, would reduce the distinctiveness of representations for each environment in hippocampus subfield CA1. Specifically, the results suggest that the patterns of input to CA1 are important for spatial distance discrimination, and this effect varies with age.

Prior research points strongly to the idea that older rats show prominent differences in several electrophysiological measures. The place cells in CA1 of aged rats show less stable firing patterns between different exposures to the same environment, suggesting that the stability of place cell firing declines with age in older rats (5, 6). Older rodents also show reduced hippocampal plasticity in the form of faster decay of long-term potentiation than do younger rodents, which is correlated with faster forgetting of spatial information in the Barnes maze (27). In the present study, we provide evidence that the stability of neural activity patterns in CA1 for the same environment was reduced in older adults (Fig. 2*E*) and was related to worse spatial distance discrimination performance (*SI Appendix*, Fig. S4). Although fMRI is an indirect measure of neural activity and cannot assay single-cell activity, our approach allowed us to image hippocampus subfield activity at higher resolution (1.6 mm × 1.6 mm × 2 mm) than many studies, with our focus on distributed populations of voxels within hippocampus subfields, which may be more closely related to the activity of ensembles of cells in rodents and monkeys (28, 29). Given the finding that age-related differences in input to CA1 mediate the stability of these patterns and their relationship to spatial distance discrimination, our results are consistent with the idea that age-associated cognitive impairments arise, in part, from underlying neurobiological changes possibly related to the stability of neural ensembles and neural plasticity.

While an accurate representation of a single environment is critical for maintaining a stable memory over time, reliable discrimination between environments is also critical for navigation. Previous findings in young humans and rodents (16, 17, 30, 31) support a role for CA1 in differentiating between spatial environments. Such findings have also been observed in memory tasks in older adults, with worse episodic memory performance being related to reductions in neural differentiation (11, 13–15, 20–23). Older rats also show reduced differentiation of neural patterns in CA3 place cells compared to younger rats (7). The degree to which neural patterns differentiate between different environments can vary across individuals even in younger adults (17). Here, we found that better performing participants in both age groups showed more distinct neural patterns for different environments, consistent with the hypothesis that greater network differentiation is related to memory accuracy regardless of age.

The correlation between increased differentiation and better spatial distance discrimination performance was mediated by the dimensionality of voxel time courses in CA1. In our present study, we observed a decrease in the dimensionality of neural signals in CA1 among older adults compared to younger adults while engaging in a spatial memory retrieval task. These effects, however, were age-invariant, suggesting that better performing older adults had behavioral performance comparable to some younger adults. The reduction in neural signal dimensionality indicates the neural activity of voxels within CA1, which in turn may have a relationship to the differentiation of codes within that subfield. One possible interpretation of this finding is that less differentiated codes in subfields such as CA1 relate to worse spatial memory performance regardless of age. Unlike our earlier mediation results, which showed an age-variant relationship between differences in input to CA1 and spatial distance discrimination performance, the mediation by voxel dimensionality effect was not related to age. The origins of such within-subfield effects are unclear, but could relate to the content of available information within brain area, which could contribute to less accurate memory performance (32). Our data suggest that richer variability in neural activity within a subfield may support better differentiation of spatial representations and more accurate spatial retrieval. Our findings also suggest that alterations in input to hippocampus CA1 contribute to the well-documented spatial memory declines with age.

We note some important limitations in our study. The first is that older adults showed within- and between-city MPS that did not differ from zero, despite using correct trials. While the same effects were present when using correct and incorrect trials, the near zero MPS for the same and different cities in older adults suggest potentially that the pattern similarity analyses may show an exaggerated group difference. In other words, given that older adults, on average, performed well at the task, it is not clear why the pattern similarity results would not be different than zero. One possibility could be the greater variability present in older adult neural patterns for the same and different cities compared to younger adults (Fig. 2*E*). Between-subject designs, such as that employed here with respect to age, involve some confounding factors, such as cohort effect and survivor effects (33). Also, the results of mediation analyses should be interpreted in light of the fact that they are based on cross-sectional data, limiting their ability to reveal the causal structure of longitudinal change (34, 35). Another limitation is our modest sample size, which could have masked some smaller-effects sizes, for example, that older adult pattern similarity values might be above zero for the same environment with sufficient data. The challenge associated with between-subject designs could be addressed in a future study using a longitudinal design involving the same older adults to examine how within- and between-city correlations might change with age. Finally, the relationship between task-related functional connectivity and underlying synaptic physiology remains unclear. As such, it is difficult to know how to interpret

the finding that PHC/PRC functional connectivity mediated the relationship between neural remapping in CA1 and spatial distance discrimination performance because functional connectivity indicates both direct and indirect connections (36). We speculate, however, that input from PHC and PRC, which may have more of a direct role in relaying sensory information (37), may be more relevant to hippocampal processing than those further along in serial processing.

Materials and Methods

Participants. Twenty-eight younger adults and twenty-five older adults were recruited from the Tucson community and the study procedures were approved by the Institutional Review Board at the University of Arizona. Written informed consent was obtained from each participant before the experiment. Three participants were excluded due to technical issues. Two participants were excluded from analysis due to too few trials after motion correction. One participant was excluded due to voluntary withdrawal during the MRI scan. The final sample consisted of 25 younger adults (14 females; mean age: 23.96 y, range: 18 to 34 y) and 22 older adults (13 female; mean age: 72.68 y, range: 65 to 82 y).

All participants were right-handed and had normal or corrected vision. Based on self-report, all participants were screened to ensure they were in good health and had no neurological or psychiatric conditions. Older adults were also screened for dementia using a battery of neuropsychological tests, including long-term memory using the California Verbal Learning Test, language using Boston Naming Test scores, speed/executive function using Trail-Making Test Parts A and B, and visuospatial abilities using Rey Complex Figure Test. Participants were considered to have MCI if they scored 1 SD below the mean on two measures within one cognitive domain (i.e., memory, language, or speed/executive function), or 1 SD below the mean on each of the three cognitive domains. All the scores showed that all older adult performance was in normative range. In addition, the Santa Barbara Sense of Direction survey (38) was adopted to measure participants' self-reported spatial and navigational abilities (*SI Appendix, Supplementary Note 1*).

Stimuli. We designed two different virtual environments using Unity3D (https://unity3d.com). Each virtual environment (i.e., city 1 and city 2) contained 6 different target stores located on the edge of the rectangular city (Fig. 1 *A*, *Left*). City 1 and city 2 shared the same basic layout, including the same ground, wall textures, and filler buildings but varied in terms of the identity of the 6 stores. Three first-person navigation videos were created for both cities (Fig. 1 *A*, *Right*). Each video contained a unique, nonrepeated navigation route.

Experimental Procedures. The experiment consisted of two sessions: a learning session outside the scanner and a retrieval session inside the scanner. During the learning session, participants were instructed to watch videos and to try to learn the store locations within each city. They were also informed there would be a spatial distance discrimination task to test whether they could successfully learn the relative distances between stores within each city. At the beginning of each round of the learning task, the participants were placed at the center of the city and viewed first-person navigation videos of travel from the center to each of the peripheral stores in a randomized order. Each learning task was followed by a shorter version (10 trials per run) of the memory retrieval task that they would later perform in the scanner (Fig. 1*C*). This learning-testing process repeated for each city in a randomized order for each participant until every participant met the criterion of 70% correct on at least one city before entering the scanner. Overall, 93.6% (N = 44) of the participants achieved 70% or higher correct responses for both cities while 6.3% (N = 3) of participants achieved 70% or higher correct responses for one city and 60% correct for the other city (see *SI Appendix*, Table S17 for more details).

The fMRI retrieval session took place in the scanner, where participants completed six retrieval runs (three per city). Each run included 20 trials involving a single city and lasted 5 min and 2 s. Before the start of each retrieval run, participants viewed one of the city refresher videos (not scanned, Fig. 1*B*) which they had seen during the learning session to remind participants of which city they would be retrieving (scanned, Fig. 1*B*) next. The order of retrieval runs was randomized across participants. For each trial, participants saw three stores on the screen for 12 s, with one store on the top and two below (Fig. 1 *C*, *Right*). Participants were asked to compare which of the two bottom stores was closer to the upper reference store and indicate their choice by pressing the corresponding key on an MR-compatible button box. A "one" response indicated that the lower-left store was closer to the top store, and a "two" indicated the lower right store was closer to the top store. A trial lasted 12 s although participants were free to respond at any time. Between trials, presentation of stimuli was jittered using a central fixation cross with an intertrial interval of 0, 3, or 6 s.

After the spatial distance discrimination task, participants were asked to complete a control task involving vowel counting, which included two runs, each containing 20 trials. The structure of each trial in the vowel counting task was the same as in the spatial distance discrimination task. Here, participants were asked to count the number of vowels (i.e., "A", "E", "I", "O", "U"; "Y" did not count) in each of the three store names and then select which of the two bottom stores had the closest number of vowels compared to the store on the top. Participants were asked to perform a vowel counting task as accurately and quickly as possible.

MRI Image Data Acquisition. Scanning was performed with a 32-Channel 3 T Siemens "Skyra" scanner located at the University of Arizona. Visual stimuli were projected onto a screen behind the scanner, which was made visible to the participant through a mirror attached to the head coil. Stimuli and responses were presented and recorded by PsychoPy (https://www.psychopy.org) on a Windows laptop. High-resolution anatomical images of the hippocampus and surrounding cortex were acquired with a T2-weighted turbo-spin echo anatomical sequence: field of view (FOV) = 200 mm × 200 mm, matrix = 448 × 448, repetition time (TR) = 4,200.0 ms, echo time (TE) = 93.0 ms, flip angle = 139°, slice thickness = 1.9 mm, 28 slices, bandwidth = 199 Hz/pixel. High-resolution functional images were acquired using a partial-brain echo planar imaging (EPI) sequence (interleaved acquisition, TR = 3,020 ms, TE = 29 ms, flip angle = 90°, FOV = 192 mm, matrix = 118 × 118, slice thickness = 2 mm, slices = 36, bandwidth = 1,462 Hz/pixel), involving a voxel resolution of 1.6 × 1.6 × 2 mm. Sequences were acquired perpendicular to the long axis of the hippocampus. High-resolution structural images of whole brain were obtained using a three-dimensional, T1-weighted Magnetization-Prepared Rapid Acquisition Gradient Echo (1 mm^3 isotropic) sequence (FOV = 256 mm, matrix = 256 × 256, slice thickness = 1 mm, TR = 1,800 ms, TE = 2.26 ms, flip angle = 8°, bandwidth = 200 Hz/pixel).

fMRI Data Preprocessing. Image preprocessing was performed by using FEAT (FMRI Expert Analysis Tool), version 6.00, implemented in FSL (part of the FSL package; http://www.fmrib.ox.ac.uk/fsl). The EPI images underwent motion correction, temporal filtering (nonlinear high-pass filter with a 100 s cutoff), and slice-timing correction. Six motion parameters were added as confound variables to the model. Residual outlier time points were identified using FSL's motion outlier detection program and integrated as additional confound variables in the first-level general linear model (GLM) analysis. No spatial smoothing was applied for single-trial estimation (see below). All functional images were linearly registered to the middle image of the first run and all analyses took place in native space.

Single-Trial Response Estimates. General linear models (GLMs) were performed separately to estimate the activation patterns for each of 120 retrieval trials. In this single-trial model, a Least Square–Separate approach was used, in which the trial of interest was modeled as one regressor, with all other trials modeled as a separate regressor. Specifically, each single-trial GLM included three regressors: 1) the trial during which a participant retrieved the spatial distance between stores; 2) all other remaining trials within the same run; and 3) the remaining time period after a participant made a judgment of all trials (i.e., 12 s minus reaction time) while the stimulus stayed on the screen (39). Each event was modeled at the time of stimulus onset and convolved with a canonical hemodynamic response function (double gamma), whereas the fixation period was not coded and thus was treated as an implicit baseline. To control for the effects of head motion, six motion parameters were included in the GLM as covariates, as well as a regressor for each TR that was flagged as having greater framewise displacement (FD) than 0.5 mm during preprocessing. These generated *t* statistics for each trial, with these *t* statistics used for MPS analyses, the PCA, functional connectivity analysis, and interregional informational connectivity analysis to increase the reliability by normalizing for noise (40). The *t* values were generated by dividing the beta value (regression fit) for each trial by the square root of the variance of residuals.

Subfield Demarcation and ROIs. Automatic hippocampus subfield segmentation software (ASHS) was used to segment the subregions of the MTL based on each participant's high-resolution T2-weighted MRI image (41, 42). We used ASHS with the ASHS-Princeton-1.0.0-Young-Adult atlas in both younger and older participants. The MTL was segmented into CA1, CA2/3, DG, and SUB, PRC, ERC, and PHC. We combined the CA2/3 and DG subfields as finer distinctions cannot be made at the acquired resolution (43). Each participant's subfield segmentations were manually inspected to ensure accuracy of both segmentation protocols. Then, each subfield ROI was transformed into each participant's native space using Advanced Normalization Tools (ANTs v2.3.5). Single-trial t-maps were then obtained within 6 ROIs (PHC, ERC, PRC, SUB, CA1, and CA2/3/DG) for each participant for further analysis.

For meaningful between-group comparisons, it was necessary to register all brains to either the old or young adult atlas. This is because comparison between different groups requires analysis within the same atlas; otherwise, spurious effects can emerge due to atlas differences alone. To verify the reliability of our results, we also performed all the same analyses by using MTL ROIs that were segmented from ASHS with the ASHS-PMC-1.0.0-Old-Adult atlas in both younger and older participants. Note that results from the Young-Adult atlas are shown in the body of the manuscript and results from the Old-Adult atlas are shown in *SI Appendix, Supplemental Text*.

MPS Analysis. MPS was applied to measure the similarity of activation patterns by calculating the correlation between trials that were correctly retrieved in each hippocampus subfield. Following the approach of Power et al., we censored volumes with a FD > 0.5 mm and excluded any trials with any censored frames during the duration of the modeled GLM response (44). Specifically, for within-city MPS, pairwise Pearson correlation coefficients were calculated by correlating correct trials of the same city with each other. All between-city MPS analyses involved correlating correct trials between different cities. All MPS analyses involved correlating trials from different runs, thus avoiding temporal autocorrelations artificially inflating or biasing results. For the within-city calculation, we excluded trials that shared all three of the same store images (for example, triads "Store 1-Store 2-Store 3" and triads "Store 1-Store 3-Store 2") to avoid identical images inflating correlations (*SI Appendix, Supplementary Note 2*). The resulting correlation coefficients were transformed into Fisher's z-scores. The SD of MPS within each condition (within-city/between-city) was then calculated to depict the stability of neural representations of MPS between two age groups. The neural remapping index was defined to be the difference between within-city and between-city MPS, i.e., within-city minus between-city MPS.

Interregional Informational Connectivity Analysis. To examine interregional informational connectivity, we calculated the correlations between the voxel patterns for 6 MTL ROIs (26, 45). First, for each ROI, we calculated the pairwise Pearson correlation among the activation patterns of trials to obtain a T-trial by T-trial representational similarity matrix (RSM, Fig. 3*A*). In this analysis, only correctly retrieved trials were included and any trials with an fMRI volume that exceeded the FD threshold of 0.5 mm were removed. Note that to exclude the effect of intrinsic fluctuations on between-ROI representation similarity, only across-run pairs of the resulting RSM were selected to conduct the second-order representation similarity analysis between the 6 ROIs (Fig. 3*B*).

In order to calculate interregional informational connectivity, we performed the following steps: 1) we included only the 5 subfields that directly input into CA1 (i.e., PHC-CA1, ERC-CA1, PRC-CA1, SUB-CA1, and CA23DG-CA1); 2) we selected the relevant edges by applying a *P*-value threshold of 0.05 (i.e., $P < 0.05$, uncorrected) to the contrast of group differences; and 3) we averaged interregional informational connectivity values to yield a single index for each participant. We calculated the interregional informational connectivity index for both the Young-Adult atlas and the Old-Adult atlas separately and identified unique subfields for each. We further used a relaxed *P*-value threshold of $P = 0.1$ to select common inputs for both atlases.

PCA. PCA was used to estimate the fidelity of voxel time courses within a subfield (46, 47). For each ROI, we extracted *t*-statistics for each correct trial, which reflected the fit of the hemodynamic response using the GLM described above. This generated a series of *t*-statistics for each voxel for all correctly retrieved trials. This N (voxels) by T (trials) matrix was then correlated with itself, generating an N-voxel by N-voxel matrix for that subfield (Fig. 4*A*). Note that similar to our MPS analysis, we also removed trials that included any volume that exceeded the FD threshold of 0.5 mm from the *t*-statistics series. Then, PCA was applied on this N by N functional connectivity matrix to obtain PCs using the MATLAB "pcacov" function (Fig. 4*A*). Finally, the dimensionality of a ROI was measured by calculating how many PCs were needed to explain 90% of variance, reflecting the potential fidelity of signals within that subfield.

For a given ROI, the maximum number of PCs is determined by the number of features (i.e., voxels). One potential issue in terms of the differences in dimensionality between two groups could be driven by the age-related differences in the number of MTL voxels. Therefore, we estimated the dimensionality by using a defined number of voxels in three different ways. First, for each MTL ROI, we obtained the voxel-wise tSNR (48) of the control task by calculating the mean of each voxel's time series divided by its SD. The voxels in each ROI could be ranked from high to low based on tSNR. After calculating each participant's number of voxels for each ROI, we selected the smallest number of voxels as the defined number of voxels M for the whole group and matched the number of voxels by selecting the top M voxels based on the tSNR intensity. We repeated this procedure for each ROI, so each ROI had a matched number of voxels, M. Second, we arbitrarily selected the top 50 voxels based on tSNR for each ROI for two reasons 1) the dimensionality of all ROIs could be compared with each other since they all involved the same number of voxels, and 2) compared to younger adults, the signal-to-noise ratio is relatively lower in older adults, and therefore, it is possible that the age-related differences in dimensionality could be driven by the noisier voxels in older adults.

Mediation Analysis. Mediation analysis was performed using version 4.2 of the PROCESS macro (49) in SPSS (V28.0.1.1) to examine whether interregional informational connectivity between MTL ROIs mediated the relationship between the neural remapping index of CA1 and spatial distance discrimination performance. We performed similar analyses using PCs. The predictor (X) is the neural remapping index in CA1, and the dependent variable (Y) is spatial distance discrimination performance. The mediators include interregional informational connectivity between MTL ROIs or the dimensionality of CA1.

Age-Variant and Age-Invariant Analysis. We systematically examined the presence of age-variant or age-invariant effects through a two-step approach. Initially, we conducted mediation analyses and/or correlation analyses without age as a covariate. In instances in which statistical significance was detected, a subsequent analysis was performed, incorporating age as a covariate. Results demonstrating sustained effects were categorized as age-invariant findings. Conversely, instances in which the observed effect was no longer significant upon the inclusion of age as a covariate were denoted as age-variant outcomes.

Statistical Analysis.

Linear mixed-effects regression. Because the number of observations (i.e., pairs of MPS) is not balanced per condition (within-city/between-city) per participant, it is more appropriate to adopt linear mixed-effects models to examine the remapping effect for younger and older adults (50). Another advantage of applying a linear mixed-effects model is that we can deal with confounding factors that could be contributing to the result on a trial-wise basis using covariates. For example, we can examine whether the differences for within-city MPS and between-city MPS were reliable after controlling for univariate activation levels and variance. Additionally, other possible confounding factors from individuals such as spatial distance discrimination performance, reaction time, and gender could also be included in the model as covariates to be regressed out.

Specifically, in R 4.2.2, we first constructed the maximal model with all possible random slopes by using the lme4 package (51). Since the maximal model did not converge successfully, we simplified the model by removing random slopes gradually until it converged (BOBYQA controller, REML estimation). Therefore, the final model included random intercepts for each participant, random slopes for ROI (PHC, ERC, PRC, SUB, CA1, and CA2/3/DG), and/or random slopes for condition (within/between-city) for each participant. The significance of the model was evaluated using Satterthwaite approximation with the lmerTest package. Post hoc tests based on the three way interactions were done using the emmeans package. We reported and plotted the estimated marginal means in the main test and figures.

Bayesian analysis. In addition to employing frequentist statistical linear mixed-effect regression, we also implemented Bayesian mixed-effects analysis to ensure the robustness of our results. We utilized the brms package (52) in R 4.2.2, employing 10 Markov chain Monte Carlo chains with 6,000 iterations per

chain, resulting in a total of 20,000 posterior iterations for coefficient estimation. Gaussian priors were employed to compute posterior medians, and we established 95% posterior credible intervals, also known as HDI, around the estimated effects. HDI that did not encompass zero were considered evidence of an effect. We also calculated the pd using bayestestR package, which acts as an indicator for the presence of an effect and has strong correspondence with the frequentist *P*-value (53). Specifically, when the pd exceeded 97.5%, it indicated the presence of an effect equivalent to a two-sided *P*-value of 0.05. When the pd exceeded 99.5%, it signified significance at a *P*-value of 0.01, and when the pd exceeded 99.95%, it demonstrated significance at a *P*-value of 0.001. Additionally, we calculated Bayesian Factors using JASP (Version 0.16.4) for all *t* tests and correlation analyses to further assess the strength of evidence for our findings. In all statistical tests, we applied a two-tailed test, and unless otherwise specified, we adopted FDR correction for multiple comparisons.

Data, Materials, and Software Availability. All data are included in the article and/or *SI Appendix* and are available on the OSF (https://osf.io/zuqhj/) (54).

ACKNOWLEDGMENTS. This research was supported by NIH/NIA grant R01 AG003376 to C.A.B. and A.D.E.

Author affiliations: [a]Psychology Department, University of Arizona, Tucson, AZ 85721; [b]Department of Psychiatry and Behavioral Sciences, Stanford University School of Medicine, Stanford, CA 94305; [c]Alzheimer's Disease Center, Department of Neurology, University of California, Davis, Sacramento, CA 95816; and [d]Evelyn F. McKnight Brain Institute, University of Arizona, Tucson, AZ 85721

Author contributions: M.F. and A.D.E designed the study; S.D. and A.O. collected the data; L.Z. analyzed data; Z.G. provided assistance with data analysis and interpretation; M.D.G. provided assistance with older adult recruitment; and L.Z., C.A.B., and A.D.E. wrote the paper.

1. A. W. Lester, S. D. Moffat, J. M. Wiener, C. A. Barnes, T. Wolbers, The aging navigational system. *Neuron* **95**, 1019–1035 (2017).
2. P. R. Rapp, M. T. Kansky, J. A. Roberts, Impaired spatial information processing in aged monkeys with preserved recognition memory. *Neuroreport* **8**, 1923–1928 (1997).
3. A. M. Daugherty, N. Raz, A virtual water maze revisited: Two-year changes in navigation performance and their neural correlates in healthy adults. *NeuroImage* **146**, 492–506 (2017).
4. S. D. Moffat, Aging and spatial navigation: What do we know and where do we go? *Neuropsychol. Rev.* **19**, 478–489 (2009).
5. C. A. Barnes, M. S. Suster, J. Shen, B. L. McNaughton, Multistability of cognitive maps in the hippocampus of old rats. *Nature* **388**, 272–275 (1997).
6. L. A. Schimanski, P. Lipa, C. A. Barnes, Tracking the course of hippocampal representations during learning: When is the map required? *J. Neurosci.* **33**, 3094–3106 (2013).
7. I. A. Wilson, S. Ikonen, M. Gallagher, H. Eichenbaum, H. Tanila, Age-associated alterations of hippocampal place cells are subregion specific. *J. Neurosci.* **25**, 6877–6886 (2005).
8. D. Marr, D. Willshaw, B. McNaughton, "Simple memory: A theory for archicortex" in *From the Retina to the Neocortex*, L. Vaina, Ed. (Birkhäuser Boston, Boston, MA, 1991), pp. 59–128.
9. M. R. Hunsaker, R. P. Kesner, The operation of pattern separation and pattern completion processes associated with different attributes or domains of memory. *Neurosci. Biobehav. Rev.* **37**, 36–58 (2013).
10. M. A. Yassa, C. E. Stark, Pattern separation in the hippocampus. *Trends Neurosci.* **34**, 515–525 (2011).
11. C. Grady, The cognitive neuroscience of ageing. *Nat. Rev. Neurosci.* **13**, 491–505 (2012).
12. J. R. Engle *et al.*, Network patterns associated with navigation behaviors are altered in aged nonhuman primates. *J. Neurosci.* **36**, 12217–12227 (2016).
13. C. L. Grady, Cognitive neuroscience of aging. *Ann. N. Y. Acad. Sci.* **1124**, 127–144 (2008).
14. D. D. Garrett, N. Kovacevic, A. R. McIntosh, C. L. Grady, The importance of being variable. *J. Neurosci.* **31**, 4496–4503 (2011).
15. C. L. Grady, Age-related differences in face processing: A meta-analysis of three functional neuroimaging experiments. *Can. J. Exp. Psychol.* **56**, 208–220 (2002).
16. L. Zheng, Z. Gao, A. S. McAvan, E. A. Isham, A. D. Ekstrom, Partially overlapping spatial environments trigger reinstatement in hippocampus and schema representations in prefrontal cortex. *Nat. Commun.* **12**, 6231 (2021).
17. C. T. Kyle, J. D. Stokes, J. S. Lieberman, A. S. Hassan, A. D. Ekstrom, Successful retrieval of competing spatial environments in humans involves hippocampal pattern separation mechanisms. *Elife* **4**, e10499 (2015).
18. R. Zhou, T. Belge, T. Wolbers, Reaching the goal: Superior navigators in late adulthood provide a novel perspective into successful cognitive aging. *Topics Cogn. Sci.* **15**, 15–45 (2023).
19. J. Y. Zhong *et al.*, The application of a rodent-based Morris water maze (MWM) protocol to an investigation of age-related differences in human spatial learning. *Behav. Neurosci.* **131**, 470 (2017).
20. L. Zheng *et al.*, Reduced fidelity of neural representation underlies episodic memory decline in normal aging. *Cereb. Cortex* **28**, 2283–2296 (2018).
21. P. F. Hill, D. R. King, M. D. Rugg, Age differences in retrieval-related reinstatement reflect age-related dedifferentiation at encoding. *Cereb. Cortex* **31**, 106–122 (2021).
22. J. D. Koen, M. D. Rugg, Neural dedifferentiation in the aging brain. *Trends Cogn. Sci.* **23**, 547–559 (2019).
23. S. L. Leal, M. A. Yassa, Neurocognitive aging and the hippocampus across species. *Trends Neurosci.* **38**, 800–812 (2015).
24. A. R. Hernandez *et al.*, Age-related impairments in object-place associations are not due to hippocampal dysfunction. *Behav. Neurosci.* **129**, 599 (2015).
25. M. A. Dalton, C. McCormick, F. De Luca, I. A. Clark, E. A. Maguire, Functional connectivity along the anterior–posterior axis of hippocampal subfields in the ageing human brain. *Hippocampus* **29**, 1049–1062 (2019).
26. N. Kriegeskorte, M. Mur, P. Bandettini, Representational similarity analysis–Connecting the branches of systems neuroscience. *Front. Syst. Neurosci.* **2**, 4 (2008).
27. C. A. Barnes, Memory deficits associated with senescence: A neurophysiological and behavioral study in the rat. *J. Comp. Physiol. Psychol.* **93**, 74 (1979).
28. N. Kriegeskorte *et al.*, Matching categorical object representations in inferior temporal cortex of man and monkey. *Neuron* **60**, 1126–1141 (2008).
29. A. D. Ekstrom, Regional variation in neurovascular coupling and why we still lack a Rosetta Stone. *Philos. Trans. R. Soc. Lond. B Biol. Sci.* **376**, 20190634 (2021).
30. I. Lee, G. Rao, J. J. Knierim, A double dissociation between hippocampal subfields: Differential time course of CA3 and CA1 place cells for processing changed environments. *Neuron* **42**, 803–815 (2004).
31. J. Stokes, C. Kyle, A. D. Ekstrom, Complementary roles of human hippocampal subfields in differentiation and integration of spatial context. *J. Cogn. Neurosci.* **27**, 546–559 (2015).
32. N. Diersch, J. P. Valdes-Herrera, C. Tempelmann, T. Wolbers, Increased hippocampal excitability and altered learning dynamics mediate cognitive mapping deficits in human aging. *J. Neurosci.* **41**, 3204–3221 (2021).
33. M. D. Rugg, "Interpreting age-related differences in memory-related neural activity" in *Cognitive Neuroscience of Aging: Linking Cognitive and Cerebral Aging*, R. Cabeza, L. Nyberg, D. C. Park, Eds. (Oxford University Press, 2017), pp. 183–203.
34. N. Raz, U. Lindenberger, Only time will tell: Cross-sectional studies offer no solution to the age–brain–cognition triangle: Comment on Salthouse (2011). *Psychol. Bull.* **137**, 790–795 (2011).
35. U. Lindenberger, T. von Oertzen, P. Ghisletta, C. Hertzog, Cross-sectional age variance extraction: What's change got to do with it? *Psychol. Aging* **26**, 34–47 (2011).
36. C. J. Honey *et al.*, Predicting human resting-state functional connectivity from structural connectivity. *Proc. Natl. Acad. Sci. U.S.A.* **106**, 2035–2040 (2009).
37. J. Erez, R. Cusack, W. Kendall, M. D. Barense, Conjunctive coding of complex object features. *Cereb. Cortex* **26**, 2271–2282 (2016).
38. M. Hegarty, A. E. Richardson, D. R. Montello, K. Lovelace, I. Subbiah, Development of a self-report measure of environmental spatial ability. *Intelligence* **30**, 425–447 (2002).
39. J. A. Mumford, B. O. Turner, F. G. Ashby, R. A. Poldrack, Deconvolving BOLD activation in event-related designs for multivoxel pattern classification analyses. *Neuroimage* **59**, 2636–2643 (2012).
40. A. Walther *et al.*, Reliability of dissimilarity measures for multi-voxel pattern analysis. *Neuroimage* **137**, 188–200 (2016).
41. P. A. Yushkevich *et al.*, Automated volumetry and regional thickness analysis of hippocampal subfields and medial temporal cortical structures in mild cognitive impairment. *Hum. Brain Mapp.* **36**, 258–287 (2015).
42. P. A. Yushkevich *et al.*, Quantitative comparison of 21 protocols for labeling hippocampal subfields and parahippocampal subregions in in vivo MRI: Towards a harmonized segmentation protocol. *Neuroimage* **111**, 526–541 (2015).
43. M. M. Zeineh, S. A. Engel, P. M. Thompson, S. Y. Bookheimer, Unfolding the human hippocampus with high resolution structural and functional MRI. *Anat. Rec.* **265**, 111–120 (2001).
44. J. D. Power, K. A. Barnes, A. Z. Snyder, B. L. Schlaggar, S. E. Petersen, Spurious but systematic correlations in functional connectivity MRI networks arise from subject motion. *Neuroimage* **59**, 2142–2154 (2012).
45. Z. Gao *et al.*, Context free and context-dependent conceptual representation in the brain. *Cereb. Cortex* **33**, 152–166 (2022).
46. Z. Gao *et al.*, Flexing the principal gradient of the cerebral cortex to suit changing semantic task demands. *Elife* **11**, e80368 (2022).
47. M. L. Mack, A. R. Preston, B. C. Love, Ventromedial prefrontal cortex compression during concept learning. *Nat. Commun.* **11**, 46 (2020).
48. K. Murphy, J. Bodurka, P. A. Bandettini, How long to scan? The relationship between fMRI temporal signal to noise ratio and necessary scan duration. *Neuroimage* **34**, 565–574 (2007).
49. A. F. Hayes, *Introduction to Mediation, Moderation, and Conditional Process Analysis: A Regression-Based Approach* (Guilford publications, 2017).
50. J. A. Mumford, R. A. Poldrack, Modeling group fMRI data. *Soc. Cogn. Affective Neurosci.* **2**, 251–257 (2007).
51. D. Bates, M. Mächler, B. Bolker, S. Walker, Fitting linear mixed-effects models using lme4. *J. Stat. Software* **67**, 1–48 (2015).
52. P.-C. Bürkner, brms: An R package for Bayesian multilevel models using Stan. *J. Stat. Software* **80**, 1–28 (2017).
53. D. Makowski, M. S. Ben-Shachar, S. H. A. Chen, D. Lüdecke, Indices of effect existence and significance in the bayesian framework. *Front. Psychol.* **10**, 2767 (2019).
54. L. Zheng, Hippocampal contributions to novel spatial learning are both age-related and age-invariant. OSF. https://osf.io/zuqhj/. Deposited 18 October 2023.